Chemical Bonding between Cu and Oxygen−Copper Oxides vs O_2 Complexes: A Study of CuO_x ($x = 0-6$) Species by Anion Photoelectron Spectroscopy

Hongbin Wu, Sunil R. Desai, and Lai-Sheng Wang*

Department of Physics, Washington State University, Richland, Washington 99352, and Environmental Molecular Sciences Laboratory, Pacific Northwest National Laboratory, MS K2-14, P.O. Box 999, Richland, Washington 99352

Received: October 14, 1996[⊗]

An extensive photoelectron spectroscopic study on the CuO_x^- ($x = 0-6$) species is presented. The photoelectron spectra of these species are obtained at four detachment photon energies: 2.33, 3.49, 4.66, and 6.42 eV. The spectra of the copper atom are included to show the dependence of the detachment cross sections on the photon energies. An intense two-electron transition to the ^2P excited state of Cu is also observed in the 6.42 eV spectrum of Cu^-. For CuO^-, we observe an excited state of the anion, as well as photodetachment transitions to charge transfer excited states of CuO ($Cu^{2+}O^{2-}$). Six transitions are observed for CuO_2^- at 6.42 eV, revealing all six valence molecular orbitals of the linear OCuO molecule. CuO_3^- is observed to undergo photodissociation at 3.49 eV to give an internally hot CuO^- plus O_2. It is shown to have an $OCuO_2$ type of structure, and its electronic structure can be viewed to be due to that of CuO perturbed by an O_2. For CuO_4^-, two isomers are observed. One of them undergoes photodissociation at 3.49 eV, and it is shown to be a Cu/O_2 complex, $Cu(O_2)_2^-$. The second isomer yields spectra identical to that of the linear $OCuO^-$ with a slight energy shift and is concluded to be an $OCuO^-$ solvated by a very weakly bonded O_2, $(OCuO^-)O_2$. CuO_6^- is shown to exhibit similar behaviors as CuO_4^- with a Cu/O_2 complex, $Cu(O_2)_3^-$, and an O_2-solvated CuO_2^-, $(OCuO^-)(O_2)_2$. The CuO_5^- spectra are observed to be similar to that of CuO_3^-, and it is shown to be due to a CuO_3^- solvated by an O_2, $(OCuO_2^-)O_2$.

I. Introduction

The chemical bonding between copper atom and oxygen is interesting both as a prototype system to understand the basic chemical bonding properties between transition metals and oxygen and due to the importance of copper in bioinorganic chemistry for dioxygen metabolism.[1,2] It is known that at room temperature Cu atom can only form mono- and bis(dioxygen) complexes, $Cu(O_2)$ and $Cu(O_2)_2$, with O_2 because the O atom transfer reaction is endothermic.[3−6] It has been shown in low-temperature matrix experiments that a copper dioxide molecule, OCuO, as well as a copper ozone complex, $Cu(O_3)$, can be formed upon UV photolysis.[6,7]

Among the Cu/O species, the copper monoxide (CuO)[8,9] and $Cu(O_2)$[3−7,10] complex are perhaps the most studied and best understood molecules both experimentally and theoretically. Several matrix experiments have observed the copper dioxide molecule,[6,7] but its structure and bonding are poorly characterized. We have previously reported on a photoelectron spectroscopy (PES) study of the $Cu(O_2)$ complex and copper dioxide, OCuO.[11,12] In the current work, we present a complete study of all the CuO_x ($x = 1-6$) species produced from a laser vaporization cluster source using size-selected anion PES. Several new Cu/O molecules are observed for the first time, and their structure and bonding information is obtained from their PES spectra taken at various detachment photon energies. Both oxides and O_2 complexes are observed for $x > 1$. We also observe wavelength-dependent photodissociations of the anions for the O_2 complexes, yielding direct structural information.

The only previous PES study was on CuO^- at 3.531 eV.[13] We obtain the CuO^- spectra at several photon energies (2.33, 3.49, 4.66, and 6.42 eV). Not only do we observe photon energy-dependent detachment cross sections of different transitions, but the high photon energies also allow transitions to higher excited states of CuO. The high excited states, representing essentially Cu 3d → O 2p charge transfer transitions, may be characterized as $Cu^{2+}O^{2-}$. Interestingly, we also observe a metastable triplet excited state of the anion that allows a new transition to CuO excited state to be observed. For CuO_2^-, the new spectrum obtained at 6.42 eV yields two extra transitions at high electron binding energies (BEs) compared to the previous spectrum at 4.66 eV that revealed four transitions.[11] The 6.42 eV spectrum represents essentially all the six valence molecular orbitals (MOs) of the linear copper dioxide molecule.

A new CuO_3^- molecule is observed for the first time, which contains a CuO^- bonded to an O_2 molecule. Its spectrum can be understood as due to that of CuO^- perturbed by an O_2 ligand. The anion of this molecule dissociates at 3.49 eV photon energy into CuO^- and O_2. We also observe a minor isomer, $Cu(O_3)^-$, that dissociates into Cu^- and O_3 at 4.66 eV. The spectrum of CuO_5^- is observed to be quite similar to that of CuO_3^-, and the observed CuO_5^- species is suggested to be CuO_3^- solvated by an O_2 molecule. For both CuO_4^- and CuO_6^-, we observe two isomers. The dominant one is due to a copper dioxide, $OCuO^-$, solvated by one and two O_2 molecules, respectively. The second isomer in both cases can dissociate to Cu^- and is due to a Cu^- bonded to two and three O_2 molecules, respectively.

The spectra of Cu^-, used as calibrations in our experiments, are obtained at several photon energies (3.49, 4.66, and 6.42 eV). Strong photon energy-dependent detachment cross sections are observed for the 4s and 3d electrons. Additionally, at 6.42 eV, a very strong two-electron transition is observed to the ^2P excited state of Cu that is produced due to strong electron correlation effects.

* To whom correspondence should be forwarded.

⊗ Abstract published in *Advance ACS Abstracts,* February 15, 1997.

S1089-5639(96)03144-1 CCC: $14.00

This paper is organized as the following. In the next section, the details of the experimental aspect will be described. The Cu^- spectra at different photon energies will also be presented and discussed in this section, showing the effects of photon energies on the PES spectra. In section III, the PES spectra of all the CuO_x^- ($x = 1-6$) species will be presented, followed by more detailed discussions of each molecule in section IV. We will present an energy level diagram for CuO^- and CuO obtained from the current work and discuss the structure and bonding between Cu and O/O_2 in the CuO_x species. A summary of the observations and conclusions is provided in section V.

II. Experimental Section

A. CuO_x^- Generation and Experimental Procedures. The CuO_x^- species are generated by pulsed laser vaporization of a pure copper target into a pulsed helium carrier gas containing from 0.05% to 5% O_2. The plasma reactions between the laser-vaporized copper atoms and the O_2 form various $Cu_nO_x^-$ clusters, which are entrained into the helium carrier gas and form a supersonic cluster beam. The species containing one copper atom is the focus of the current paper. The most abundant CuO_x^- species is always CuO_2^- over the range of the O_2 concentrations used. CuO^- is produced more easily at the lowest O_2 concentration. The abundance of the higher CuO_x^- species decreases as x increases, and the maximum x is observed to be 6, which can only be produced in appreciable abundance for the PES experiments when the 5% O_2/He carrier gas is used.

The magnetic-bottle time-of-flight (MTOF) photoelectron spectrometer has been described in detail previously.[14] Briefly, the negative clusters are extracted from the collimated cluster beam after one skimmer at 90° and are mass-analyzed by a TOF mass spectrometer. The cluster of interest is selected by a pulsed mass gate and decelerated by a momentum decelerator before crossing with a detachment laser beam in the MTOF interaction zone. The photoelectrons are collected by the magnetic bottle at nearly 100% efficiency and are energy-analyzed by their time of flight in a 3.5 m long TOF tube.[15] In the current work, both a Q-switched Nd:YAG laser [532 nm (2.33 eV), 355 nm (3.49 eV), and 266 (4.66 eV) nm] and an excimer laser [193 nm (6.42 eV)] are used for photodetachment. At 4.66 and 6.42 eV, spectra are taken at 20 Hz with the cluster beam off at alternating shot for background subtraction. The electron TOF spectra are converted to electron kinetic energy distributions calibrated by the known spectra of Cu^- and smoothed with a 5 or 10 meV square window function. The kinetic energy spectra are subtracted from the respective detachment photon energies to obtain the electron binding energy spectra presented. The resolution of the spectrometer is better than 30 meV at 1 eV kinetic energy. The best resolution is obtained when low photon energies are used. However, high photon energies allow more deeply bonded electrons to be probed.

B. Cu^- PES at 3.49, 4.66, and 6.42 eV: Photon Energy Dependence and Observation of a Strong Two-Electron Transition. Figure 1 shows the Cu^- spectra at three photon energies that are used as calibrations for the TOF-to-kinetic energy conversions. The 355 nm spectrum in Figure 1 represents the best resolution of our spectrometer. The peak widths (fwhm) for the $^2S_{1/2}$, $^2D_{3/2}$, and $^2D_{1/2}$ states are 47, 22, and 19 meV, respectively, showing the resolution dependence on the electron kinetic energies. This dependence is also shown clearly from the increasing peak widths for the 266 and 193 nm spectra. The bandwidth of the excimer laser (~20 meV) also contributes to the broadening of the 193 nm spectrum. From Figure 1, it can be seen clearly that the noise begins to show up at the high BE side of the 266 nm spectrum above ~3.5 eV

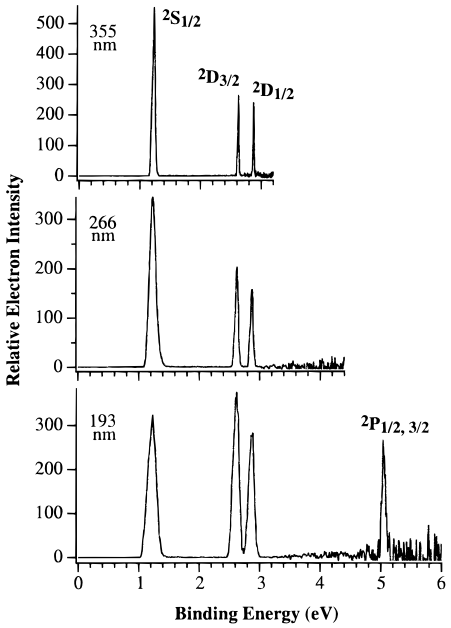

Figure 1. Photoelectron spectra of Cu^- at 355, 266, and 193 nm.

BE. The 193 nm spectrum indicates that the noise becomes significant above 4.6 eV BE, and often low photon fluences have to be used at the higher photon energies to reduce the noise problem.

We also observe two other new features in Figure 1: (1) the photon energy dependence of detachment cross sections for different transitions and (2) a new peak near 5 eV BE at 193 nm. Since our spectrometer collects nearly 100% of the photoelectrons, the relative peak intensities represent the relative total detachment cross sections. We observe that the cross section for the ^2D states increases with photon energies relative to that for the ^2S state. This is consistent with the general observation in PES that cross sections for emitting electrons from higher angular momentum states increase with photon energies.[16]

The new peak observed at 5 eV BE is interesting since it is due to a two-electron transition. This peak can be assigned from the Cu atomic energy levels.[17] It is due to the ^2P excited state of Cu atom with an $3d^{10}4p^1$ electron configuration. There is a small spin−orbit splitting (30 meV)[17] that is not resolved in the 193 nm spectrum. Cu^- has a $3d^{10}4s^2$ configuration. Thus, the ^2P state resulted from detaching a 4s electron and at the same time exciting another 4s electron to the 4p orbital. Such two-electron transitions are common in PES, which is the chief experimental technique to study electron correlation effects in atoms and molecules.[18] These transitions are usually called satellites and exhibit very weak intensities. It is surprising that the intensity of the ^2P state observed here are almost comparable to the main transitions. This suggests very strong electron correlation effects between the two 4s electrons in Cu^-.

Figure 1 shows the advantages of performing PES experiments at various photon energies using the MTOF technique. Low photon energies allow optimum spectral resolution and are noise-free while high photon energies can reveal more highly excited states. Additionally, photon energy dependence of detachment cross sections can provide useful information in spectral assignments concerning the initial states of the photoemitted electrons.

III. Results

The PES spectra of CuO_x^- are displayed in Figures 2−7 for $x = 1-6$, respectively. The spectra of CuO^- are taken at four

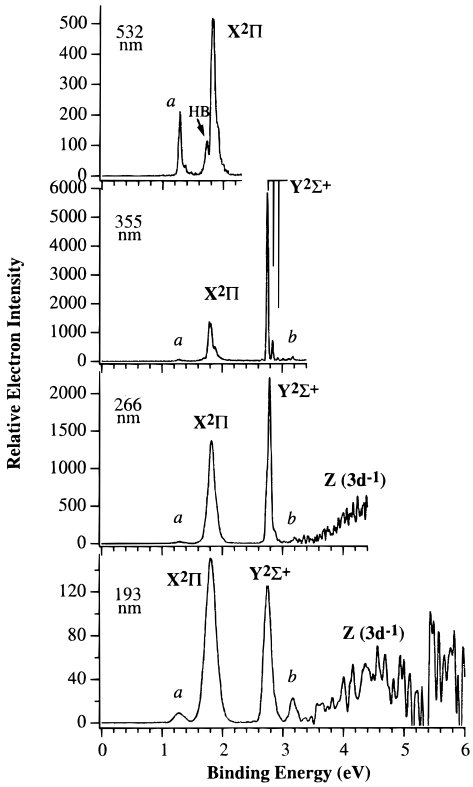

Figure 2. Photoelectron spectra of CuO^- at 532, 355, 266, and 193 nm. HB stands for hot band transitions.

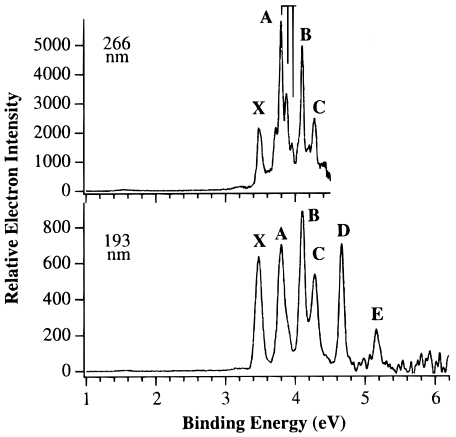

Figure 3. Photoelectron spectra of CuO_2^- at 266 and 193 nm.

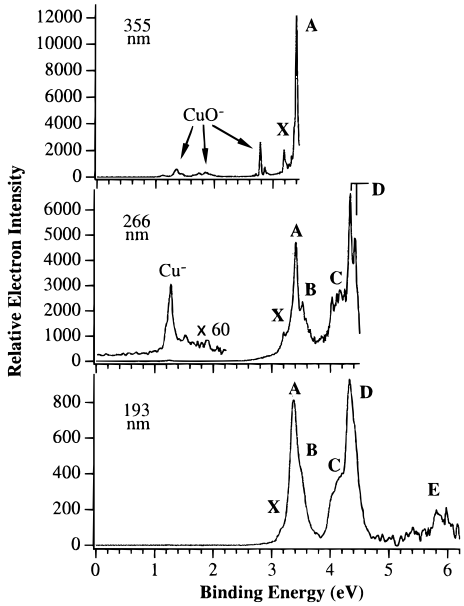

Figure 4. Photoelectron spectra of CuO_3^- at 355, 266, and 193 nm.

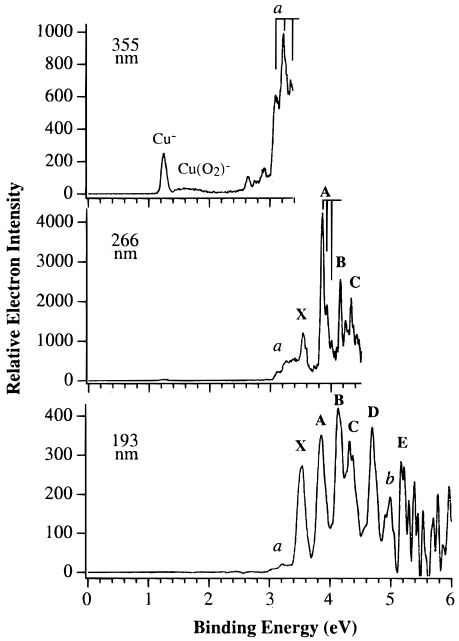

Figure 5. Photoelectron spectra of CuO_4^- at 355, 266, and 193 nm.

photon energies, each revealing more transitions (Figure 2). There are two major features labeled as X and Y, two weak features labeled as *a* and *b*, and a broad band starting near 4 eV BE labeled as Z. The X band at 532 nm shows clear hot band transitions. The Y band at 355 nm is vibrationally resolved. The broad feature labeled Z is partially observed at 266 nm. It is fully observed at 193 nm although the spectrum becomes rather noisy at the high BE side. The CuO_2^- spectra are shown at two photon energies in Figure 3. At 266 nm, four bands are observed and are labeled as X, A, B, and C. The A band contains clear vibrational structures. At 193 nm, two new features are observed and are labeled as D and E.

For CuO_3^- to CuO_5^-, each is studied at three photon energies (Figures 4−6). The spectra of CuO_6^- (Figure 7) are only taken at two photon energies with relatively low counting rate because the CuO_6^- anion mass abundance is rather weak. This makes it very difficult to measure the PES spectrum at 193 nm due to the severe noise problem. For CuO_3^- (Figure 4), the 355 nm spectrum shows surprisingly features due to CuO^- besides the features labeled as X and A due to CuO_3^-. This is compared to the spectrum of CuO^- in Figure 8 on the same BE energy scale, where the peak labeled A in Figure 4 is not shown. And the feature near 3.2 eV that is labeled X in Figure 4 clearly overlaps with the feature labeled as *b* in the CuO^- spectrum. Additionally, the CuO^- spectrum from the CuO_3^- beam shows significant hot band transitions and an extra feature labeled as *a′* in Figure 8. At 266 nm, more features are observed and are labeled as B, C, and D (Figure 4). However, the CuO^- features that show up in the 355 nm disappear in the 266 nm spectrum. A close examination reveals that there is a very weak feature near 1.23 eV BE that can be attributed to Cu^-. Both the Cu^- and CuO^- features must be due to photodissociations of the parent CuO_3^- anions and subsequent detachment of the anion product by a second photon from the same detachment laser pulse (see below). The photodissociations appear to be wavelength dependent. At 193 nm, no signals that can be attributed to either Cu^- or CuO^- are observed, and a weak feature at high BE near 5.8 eV, labeled as E, is observed.

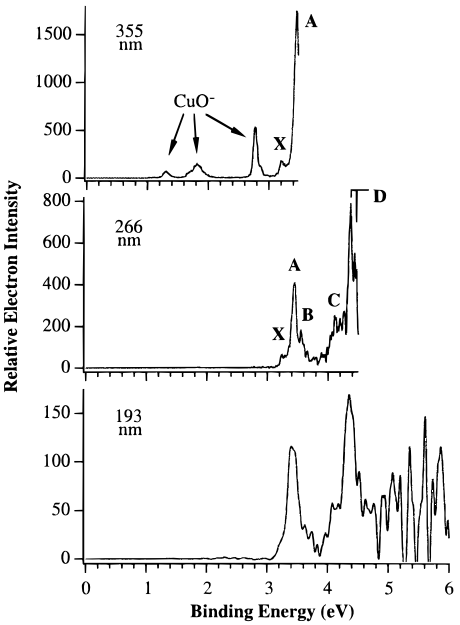

Figure 6. Photoelectron spectra of CuO_5^- at 355, 266, and 193 nm.

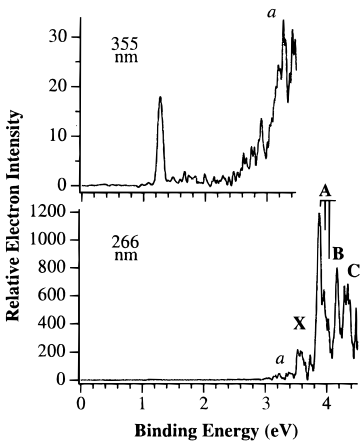

Figure 7. Photoelectron spectra of CuO_6^- at 355 and 266 nm.

For CuO_4^- (Figure 5), the 355 nm spectrum shows features that can be attributed to both Cu^- and $Cu(O_2)^-$ complex beside the vibrationally resolved feature labeled as *a*. At 266 nm, several new features are observed (X, A, B, C), and the A band is also vibrationally resolved. The features due to Cu^- and $Cu(O_2)^-$ complex are almost negligible, and the feature *a*, observed at 355 nm, is seen not to be the dominant one compared to the features labeled as X, A, B, and C. Surprisingly, these features are nearly identical to that of the copper dioxide spectrum shown in Figure 3, except that there is a small BE shift of about 0.06 eV. The 193 nm spectrum is also similar to that of CuO_2^- except that there is a new feature near about 5 eV (labeled as *b*) for CuO_4^-. Even the vibrational frequency of the A band for CuO_4^- is identical to that of CuO_2^-. The spectra of CuO_6^- (Figure 7) show similar patterns to that of CuO_4^-, and the 266 nm spectrum shows no measurable shift compared to that of CuO_4^-. Figure 9 displays the 266 nm spectra of CuO_2^-, CuO_4^-, and CuO_6^- on the same energy scale, and the similarity of the spectra is clearly shown.

The spectra of CuO_5^- (Figure 6) show striking similarities to that of CuO_3^- (Figure 4). At 355 nm, again features due to CuO^- are observed in the CuO_5^- spectrum. The major features of the CuO_5^- spectrum (X, A, B, C, and D) exhibit a slight shift in BE relative to that of CuO_3^-. The 193 nm spectrum of CuO_5^- has poor statistics due to the weak CuO_5^- mass

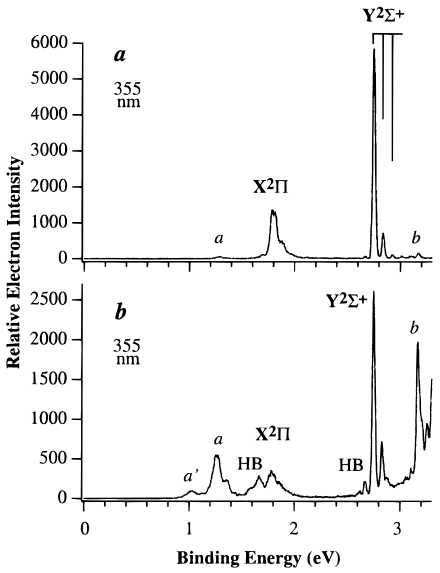

Figure 8. (a) CuO^- spectrum at 355 nm, same as in Figure 2. (b) Hot CuO^- spectrum at 355 nm from dissociation of CuO_3^-, same as in Figure 4. Figure HB stands for hot band transitions.

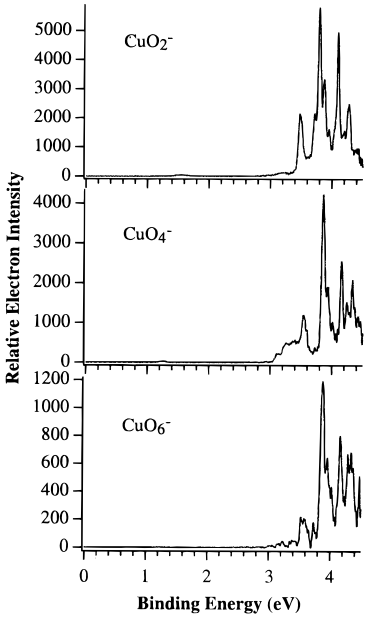

Figure 9. Comparison of the 266 nm spectra of CuO_2^-, CuO_4^-, and CuO_6^-.

abundance. Nevertheless, it reproduces all the features at 266 nm, and its similarity to that of CuO_3^- is well revealed. Figure 10 shows the spectra of CuO_5^- and CuO_3^- along with that of CuO^-.

The BEs of all the observed features and the obtained spectroscopic constants are listed in Table 1−6 for CuO_x^- ($x = 1-6$), respectively. In the following, each CuO_x species is discussed individually.

IV. Discussion

A. CuO. Many theoretical and experimental works have been devoted to the electronic structure and spectroscopy of CuO, which may be viewed as $Cu^+(3d^{10})O^-(2p^5)$ with a valence configuration of $3d\sigma^2 3d\pi^4 3d\delta^4 2p\sigma^2 2p\pi^3 4s\sigma^0$ ($X^2\Pi$) where the empty $4s\sigma$ MO is mainly the Cu 4s orbital.[8,9] In the anion, the extra electron enters the $2p\pi$ orbital, resulting in a closed-shell ground state for the CuO^- anion ($X^1\Sigma^+$), which can be roughly described as $Cu^+(3d^{10})O^{2-}(2p^6)$. Removal of a $2p\pi$ electron

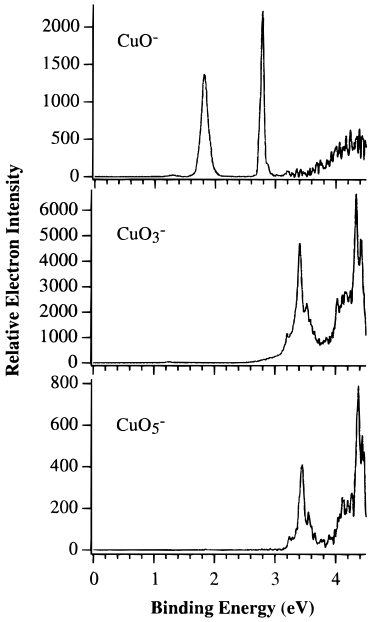

Figure 10. Comparison of the 266 nm spectra of CuO^-, CuO_3^-, and CuO_5^-.

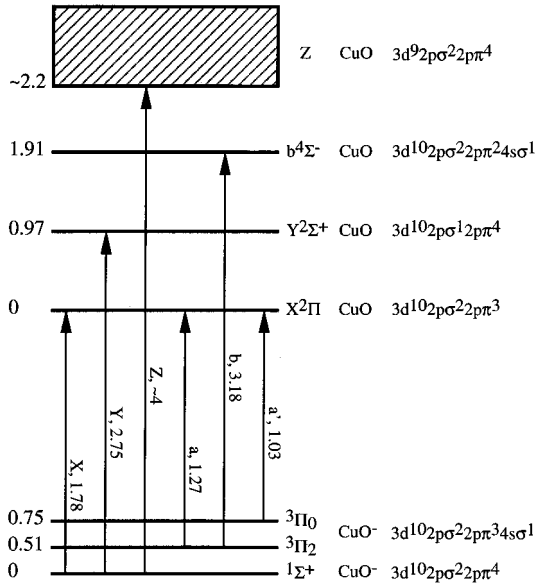

Figure 11. Schematic diagram of the energy levels of CuO^- and CuO and the photodetachment transitions. Energies are in eV.

leads to the $X^2\Pi$ ground state of CuO at a BE of 1.78 eV while detaching a 2pσ electron gives rise to the $Y^2\Sigma^+$ state at a BE of 2.75 eV (Figure 2). Both of these states have been well discussed in the previous PES work that also had better resolution.[13] The spin−orbit splitting of the $X^2\Pi$ ground state (277 cm^{-1}) was well resolved in the previous work while it is not resolved in Figure 2. Therefore, we will only focus on the new observations in the current work, including the relative intensity changes of the X and Y states at different photon energies, the features labeled as *a* and *b*, and the features at high photon energies labeled as Z. The electron affinity (EA) and the X−Y separations obtained presently (Table 1) agree well with the previous study.[13]

Figure 2 indicates that the intensity of the X band increases with photon energies relative to the Y band. Photoemission cross sections for high angular momentum states in general increase with photon energies.[16] The photon energy dependence of the relative intensities of the X and Y bands is consistent with their orbital characters, an indirect support for their assignments.

The observations of the *a* and *b* features are surprising since they were not observed in the previous work.[13] At first glance, feature *a* can be due to two sources: from either an impurity in the CuO^- anion beam or an electronic excited state of CuO^-. Our TOF mass spectrometer has a mass resolution of about 500 ($M/\Delta M$) that is sufficient to resolve impurities like O_5^- or $CuOH^-$ from CuO^-.[14,19] Furthermore, we have obtained PES spectrum of $CuOH^-$ that gives a quite different PES spectrum compared to features *a* and *b*.[20] The mass of CuO^- coincides with the two isotopes of Br^-. However, Br^- has a different PES spectrum,[21] and moreover, there is no source of Br^- in our cluster source any way. Therefore, we assign the feature *a* to be due to an electronically excited state of CuO^-. Additionally, its intensity depends on source conditions, consistent with this assignment. For the 532 nm spectrum, the CuO^- beam was seemingly hot, judging by the significant hot band transition on the low BE side of the X band. The feature *a* is also observed to be very strong in the 532 nm spectrum. Both features *a* and *b* must be due to the same origin because their intensities depend on the source conditions in the same fashion. In both the 355 and 266 nm spectra shown in Figure 2, the CuO^- beam was quite cold without any substantial hot band transitions. In these cases, the population of the electronically excited state of CuO^- is also observed to be low as seen by the low intensities of the features *a* and *b* in these two spectra. As will be shown in the following when CuO_3^- is discussed, very hot CuO^-, both vibrationally and electronically, can be produced from photodissociation of CuO_3^- at 355 nm (Figure 8).

Observation of excited states for anions is rare. However, they have been observed in another transition metal monoxide (FeO).[22] Recently, calculations have predicted excited triplet states for several cluster anions.[23] The lowest excited state for CuO^- would be to excite a 2pπ electron to the empty 4sσ orbital, giving a triplet excited state $3d\delta^4 3d\pi^4 3d\sigma^2 2p\sigma^2 2p\pi^3 4s\sigma^1$ ($^3\Pi$). This suggests that when the CuO^- anion is formed there is a finite probability for the extra electron to enter the 4sσ orbital to give the metastable $^3\Pi$ excited state, which can be roughly viewed as $Cu(3d^{10}4s^1)O^-(2p^5)$, i.e., Cu^0O^-. This is equivalent to a charge transfer transition from the ground state Cu^+O^{2-} anion to a Cu^0O^- anion (O 2p → Cu 4s). From the BE of the feature *a*, this excitation energy is 0.51 eV. The feature *a* is then formed by a transition from the excited CuO^- anion to the ground state of CuO, i.e., by removing the 4sσ electron in the photodetachment transition. Detachment of a 2pπ electron from the excited CuO^- anion will lead to a quartet excited state for CuO ($3d\delta^4 3d\pi^4 3d\sigma^2 2p\sigma^2 2p\pi^2 4s\sigma^1$, $^4\Sigma^-$). We assign the feature *b* to this transition. This gives an excitation energy of 1.91 eV above the CuO ground state. A quartet state has been observed and assigned to CuO in previous optical experiments with a similar excitation energy. However, a different electron configuration was assigned.[9] In light of the current observation, this previous assignment needs to be reevaluated. An energy diagram is presented in Figure 11, showing the transitions resulting in the features X, Y, *a*, and *b*, as well as the features Z and *a*′ which will be discussed below.

The 266 nm spectrum of CuO^- shows a tail of broad band at high BE (~4 eV). This band is seen to extend to about 5 eV in the 193 nm spectrum. The broad nature of this band is unusual and suggests that there is a significant geometry change from the anion to the neutral. From the ground state configuration of CuO^-, this band is likely to be due to detachment of the 3d electrons ($3d\delta^4 3d\pi^4 3d\sigma^2$). This will result in excited states which may be viewed as $Cu^{2+}O^{2-}$, i.e., 3d(Cu) → 2p(O) charge transfer states. Both Cu and O atoms are in valence

TABLE 1: Observed Binding Energies (BE) and Spectroscopic Constants for CuO^- and CuO

	state	BE (eV)[a]	term value (eV)[b]	vib freq (cm^{-1})[b]
CuO^-	X ($^1\Sigma^+$)	0	0	640 (80)
	a ($^3\Pi_2$)	1.27	0.51 (2)	
	a′ ($^3\Pi_0$)	1.03	0.75 (3)	
CuO	X ($^2\Pi$)	1.78	0	640 (80)
	Y ($^2\Sigma^+$)	2.75	0.97 (2)	
	b ($^4\Sigma^-$)	3.18	1.91 (2)	
	Z ($3d^{-1}$)	∼4	∼2.2	

[a] Uncertainty ±0.04 eV. [b] Relative energies can be determined more accurately.

TABLE 2: Observed Binding Energies (BE) and Spectroscopic Constants for CuO_2^- and CuO_2

	state	BE (eV)[a]	term value (eV)[b]	vib freq (cm^{-1})[b]
$OCuO^-$	X ($^1\Sigma_g^+$)	0		600 (80)
OCuO	X ($^2\Pi_g$)	3.47	0	
	A	3.79	0.32 (2)	640 (80)
	B	4.10	0.63 (2)	640 (80)
	C	4.28	0.81 (2)	
	D	4.67	1.20 (2)	
	E	5.16	1.69 (2)	

[a] Uncertainty ±0.04 eV. [b] Relative energies can be determined more accurately.

two in these excited states compared to valence one in the ground state. This change of bonding character is expected to lead to shorter bond length in the excited states, resulting in the broad PES spectrum. Previous calculations predicted that such charge transfer states should occur 10 000−30 000 cm^{-1} above the ground state.[8,10] This agrees with our observation.

Table 1 summarizes all the spectroscopic constants and the electron binding energies obtained from the current work for CuO and CuO^-. Figure 11 shows a schematic diagram of all the observed energy levels for CuO and CuO^- and the photodetachment transitions that result in the features observed in Figures 2 and 8 (see below in the discussion of CuO_3^- for the assignment of the feature *a′*). It would be interesting to perform accurate *ab initio* calculations on the possible excited states of the CuO^- anion to confirm the spectral assignment and interpretation. The observation of the $Cu^{2+}O^{2-}$ type of excited states is also interesting and warrants more accurate calculations that may help elucidate the nature of the Cu−O bonding completely.

B. CuO_2. CuO_2 has two isomers, a $Cu(O_2)$ complex and a copper dioxide, OCuO.[3−7,10] We have reported the CuO_2^- PES spectra at 355 and 266 nm previously.[11] Both isomers were observed, and the $Cu(O_2)^-$ complex was shown to dissociate to $Cu^- + O_2$ at 355 nm. We refer the readers to the previous publication for details. We include CuO_2 in this discussion for completeness and also report a new spectrum at 193 nm which allows two new transitions (D and E, Figure 3) to be observed. The vibrational structure on the A state at 266 nm is better resolved currently, and a resolved hot band transition at the low BE side of the A band yields a vibrational frequency of 600 cm^{-1} for the ground state of the copper dioxide anion. In the previous work, we show that the electronic structure of the OCuO dioxide can be viewed as a $Cu^{2+}(3d^9)$ interacting with two $O^-(2p^5)$. In the linear geometry, this results in six valence MOs with a doublet ground state, $1\delta_g^4 1\pi_u^4 2\pi_u^4 1\sigma_g^2 2\sigma_g^2 1\pi_g^3$ ($X^2\Pi_g$). In the anion, the extra electron enters the $1\pi_g$ orbital, giving a closed-shell ground state for the CuO_2^- anion, $1\delta_g^4 1\pi_u^4 2\pi_u^4 1\sigma_g^2 2\sigma_g^2 1\pi_g^4$ ($X^1\Sigma_g^+$). There has been only one previous calculation on the copper dioxide molecule, and its electronic structure is not well understood.[12] The 193 nm spectrum shown in Figure 3 reveals all the six valence MOs with each peak corresponding to one of the six MOs. However, we cannot assign the exact ordering of these orbitals. From the relative intensity changes of the X and A bands from the 266 to 193 nm spectra, we can infer that the X band corresponds to a state with higher angular momentum than the A state. This is consistent with the X and A states as resulting from a π and σ orbital, respectively.

TABLE 3: Observed Binding Energies (BE) and Spectroscopic Constants for CuO_3

	state	BE (eV)[a]	vib freq (cm^{-1})[b]
$OCuO_2$	X	3.19	
	A	3.39	
	B	3.51	
	C	4.02	
	D	4.34	660 (90)
	E	∼5.8	

[a] Uncertainty ±0.04 eV. [b] Relative energies can be determined more accurately.

C. CuO_3. The PES spectra of CuO_3^- are shown in Figure 4 at three photon energies. The 355 nm spectrum shows an intense sharp peak at 3.39 eV labeled as A and a weak peak at 3.19 eV labeled as X. The rest of the features can all be attributed to CuO^-. At 266 nm, more features at higher BE are revealed, B, C, and D, while the features due to CuO^- disappear. A very weak feature (note the ×60 amplification) near 1.23 eV is observed. At 193 nm, all the features observed at 266 nm (X−D) are reproduced and, additionally, there is a weak feature near 5.8 eV labeled as E. In the 266 nm spectrum, vibrational structure is clearly resolved in the D band with a frequency of 660 cm^{-1} (Table 3). The C band also contains vibrational structures, but no regular progression can be identified. The feature B is separated from A by 0.12 eV and could be due to a vibrational level above A, but no higher members can be identified even though there are clearly features above B. The feature X is rather weak but is clearly present in all three spectra. We assign it as the ground state of the CuO_3^-, yielding an EA of 3.19 eV for CuO_3 neutral.

The observation of CuO^- features in the 355 nm spectrum of CuO_3^- is due to photodissociation of the parent CuO_3^- anion, $CuO_3^- \rightarrow CuO^- + O_2$, and subsequent photodetachment of the CuO^- product by a second photon from the same detachment laser pulse (7−10 ns pulse width). This dissociation is wavelength dependent and only occurs efficiently at 355 nm. Similar dissociation event takes place in the $Cu(O_2)^-$ complex, which also only dissociates at 355 nm.[11] This suggests that the O_2 unit is the chromophore that absorbs the 355 nm light. We conclude that the CuO_3 molecule must also contain an O_2 unit bonded to a CuO unit, i.e., $OCuO_2$, which may be viewed as replacing an O atom in OCuO by an O_2 unit. This CuO_3 molecule has never been observed or calculated before, and its electronic structure is not known. Therefore, it is not possible here to assign all the observed electronic states in detail. The bonding between O_2 and CuO in CuO_3 is substantial since the EA of CuO_3 (3.19 eV) is increased significantly compared to CuO (1.78 eV). In analogy to OCuO, the CuO_3 molecule may be regarded as $O^-Cu^{2+}(O_2)^-$. The electronic states of the CuO_3 molecule seem to group into two regions: one including features X, A, and B and the other C and D. These two groups can be viewed as derived from the X and Y states of CuO perturbed by an O_2 molecule. Indeed, the separation between the two groups of states in CuO_3 is very similar to that between the X and Y states in CuO (Figure 10). This also suggests that all these features from X to D are due to the O 2p orbitals as the X and Y states are in CuO. The high BE feature, E, observed at 193 nm is most likely due to the Cu 3d orbitals. Therefore,

the O_2 perturbation in CuO_3 shifts all the corresponding features in CuO to high BE by about 1.5 eV in CuO_3.

The weak feature near 1.23 eV in the 266 nm spectrum is due to Cu^-, which must be from photodissociation, $CuO_3^- \rightarrow Cu^- + O_3$, and subsequent photodetachment of the product Cu^-. However, this dissociation is not observed at 355 nm. This suggests that there is another isomer in the CuO_3^- beam that may be depicted as $Cu(O_3)^-$ or a Cu/ozone complex. Such a complex has been observed in previous matrix experiments when the Cu/O_2 matrix was photolyzed.[6] From the weak intensity of the Cu^- peak, we infer that the abundance of this complex in our CuO_3^- beam is very small. There are no direct detachment transitions that can be attributed to the $Cu(O_3)^-$ complex because of its weak abundance. The signals in the high BE side of the $\times 60$ portion of the spectrum may be due to the direct detachment transitions from $Cu(O_3)^-$ since the EA of such a complex is expected to be similar to $Cu(O_2)$ complex which occurs near this spectral region.[11]

The spectrum of CuO^- from photodissociation of CuO_3^- is compared in Figure 8 to that of the direct CuO^- spectrum in the same energy scales. It is immediately clear that the dissociation product CuO^- is vibrationally very hot as shown in the significant hot band transitions. It is also electronically hot as seen from the strong intensities of the features *a* and *b*. The feature *b* in Figure 8b overlaps with the feature X of CuO_3^- itself. Interestingly, Figure 8b also reveals an extra feature, *a′*, at a very low BE of about 1 eV. We assign this feature to be from a more highly excited state of the CuO^- anion. This is possible because of the considerable internal energy partitioned to CuO^- from the CuO_3^- dissociation. In the above, we assigned the feature *a* to be due to a $^3\Pi$ excited state of CuO^-. This state should exhibit a spin−orbit splitting to two components: $^3\Pi_2$ and $^3\Pi_0$. This splitting is expected to be large since it is mostly derived from the Cu 4s orbital. We assign the *a* feature to be due to the $^3\Pi_2$ state and the *a′* to be due to the $^3\Pi_0$ component (Figure 11). This gives a spin−orbit splitting of 0.24 eV (Table 1), which is comparable to the spin−orbit splitting in the ^{2}D state of Cu atom (0.253 eV, Figure 1).[17] This suggests that the higher spin−orbit component, $^3\Pi_0$, is only populated in the dissociation product, $CuO_3^- \rightarrow CuO^- + O_2$. Alternatively, the feature *a′* may be assigned to be from a $^1\Pi$ excited state of CuO^- anion. We cannot definitively assign this state without accurate theoretical calculations on the electronic states of the CuO^- anion.

D. CuO_4 and CuO_6. The spectra of CuO_4^- are obtained at three photon energies and are shown in Figure 5. The 355 nm spectrum shows a strong band at 3.09 eV BE, labeled as *a*, and other low BE features that are due to Cu^- and $Cu(O_2)^-$. The *a* band is vibrationally resolved with a frequency of about 1010 cm^{-1}. At 266 nm, several new features are observed, X, A, B, and C, and the *a* band is observed not to be the dominant feature. The A band is vibrationally resolved with a frequency of 640 cm^{-1}. At 193 nm, three more features are further revealed, D, *b*, and E, although the spectrum at high BE is quite noisy. Interestingly, the Cu^- and $Cu(O_2)^-$ signals due to photodissociations of the parent CuO_4^- are negligible in the 266 and 193 nm spectra.

The features observed in the 266 nm spectrum (X, A, B, C) are identical to the spectrum of the $OCuO^-$ anion (Figure 3), except that each feature is shifted to higher BE by 0.06 eV (Table 4). Even the vibrational frequency observed for the A band is identical to that in $OCuO^-$. The 193 nm spectrum of CuO_4^- is also identical to that of $OCuO^-$, except the features *a* and *b*. Therefore, we assign the major features (X, A, B, C, D, E) to be due to a copper dioxide solvated by an O_2 molecule, $(OCuO^-)O_2$. The 0.06 eV shift in BE is then due to the O_2 solvation effect. Here the O_2 is shown to have very little perturbation to the OCuO molecule, unlike the O_2 interaction with CuO in $OCuO_2$.

TABLE 4: Observed Binding Energies (BE) and Spectroscopic Constants for CuO_4

	state	BE (eV)[a]	vib freq (cm^{-1})[b]
$(O_2)Cu(O_2)$	a	3.09	1010 (90)
	b	4.99	
$OCuO(O_2)$	X	3.53	
	A	3.85	640 (80)
	B	4.16	640 (80)
	C	4.34	
	D	4.71	
	E	5.20	

[a] Uncertainty ±0.04 eV. [b] Relative energies can be determined more accurately.

Since we know that the copper dioxide molecule does not dissociate under our experimental conditions, the observation of Cu^- and $Cu(O_2)^-$ at 355 nm must be due to photodissociations of another CuO_4^- isomer. The feature labeled, *a*, then represents the direct photodetachment transitions from this isomer. Again, we observe that this dissociation is wavelength dependent since there is little dissociation observed at the higher photon energies. This isomer is less abundant compared to the $(OCuO^-)O_2$ isomer. We know from both CuO_2^- and CuO_3^- the isomers containing an O_2 unit tend to absorb at 355 nm and undergo efficient dissociation. This suggests that the CuO_4^- isomer contains two O_2 units for which we designate $(O_2)Cu(O_2)^-$. The 1010 cm^{-1} vibrational frequency observed in the *a* band must be due to an O−O stretching mode. In the 266 nm spectrum, we do not observe any other transitions that can be attributed to this isomer beside the feature *a*. In the 193 nm spectrum, an extra feature, labeled as *b*, is observed that is not due to the $(OCuO^-)O_2$ complex. We attribute this feature to the $(O_2)Cu(O_2)^-$ isomer.

The CuO_6^- mass abundance is quite low. We are only able to take its spectra at 355 and 266 nm, which are shown in Figure 7. The 355 nm spectrum has rather low counting rate. Interestingly, both of these spectra are quite similar to the CuO_4^- counterparts. The 355 nm spectrum again show features of Cu^- that must be due to photodissociation of the parent CuO_6^- anion. The 266 nm spectrum is identical to that of CuO_4^- and shows no energy shift within our experimental uncertainty relative to the features of CuO_4^-. In analogy to CuO_4^-, we conclude that CuO_6^- also has two isomers. The dominant one yields the features X, A, B, C and can be described as a copper dioxide/O_2 complex, $(OCuO^-)(O_2)_2$. The vibrational frequency observed here in the A band is also identical to that in OCuO. The other isomer which is much less abundant gives the feature *a* and dissociates into Cu^- at 355 nm. This isomer is due to a Cu/O_2 complex, $Cu(O_2)_3^-$. The spectra of CuO_2^-, CuO_4^-, and CuO_6^- at 266 nm are compared in Figure 9, and their similarity is obvious.

E. CuO_5. The spectra of CuO_5^- shown in Figure 6 also exhibit striking similarity to the CuO_3^- counterparts. The spectral features show a slight shift to higher BE (Table 5). The vibrational frequency resolved in the feature D is also identical to that as in CuO_3^-. This suggests that CuO_5^- is a CuO_3^- solvated by a molecular O_2, $(OCuO_2^-)O_2$. The second O_2 apparently is much more weakly bonded than the first O_2 in CuO_3 since the second O_2 perturbs the CuO_3 spectrum very slightly. The 266 nm spectrum of CuO_5^- is compared to that of CuO_3^- in Figure 10 along with the CuO^- spectrum.

F. The Structure and Bonding of CuO_x ($x = 1-6$). Figure 12 summarizes all the isomers and the proposed structures for

TABLE 5: Observed Binding Energies (BE) and Spectroscopic Constants for CuO_5

	state	BE (eV)[a]	vib freq (cm^{-1})[b]
$OCuO_2(O_2)$	X	3.21	
	A	3.43	
	B	3.55	
	C	4.05	
	D	4.39	660 (80)

[a] Uncertainty ±0.04 eV. [b] Relative energies can be determined more accurately.

TABLE 6: Observed Binding Energies (BE) and Spectroscopic Constants for CuO_6

	state	BE (eV)[a]	vib freq (cm^{-1})[b]
$Cu(O_2)_3$	a	~3.2	
$OCuO(O_2)_2$	X	3.53	
	A	3.87	640 (90)
	B	4.17	
	C	4.34	

[a] Uncertainty ±0.04 eV. [b] Relative energies can be determined more accurately.

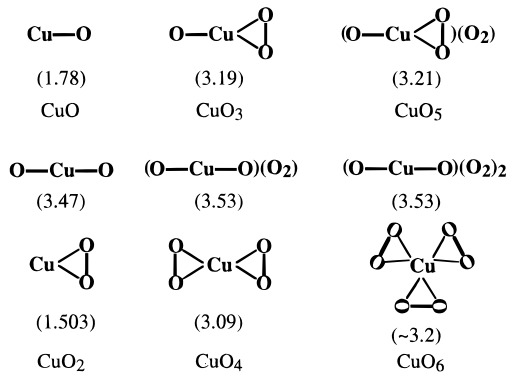

Figure 12. Schematic diagram of the structures and isomers of the CuO_x ($x = 1-6$) species. The numbers in the parentheses are the corresponding electron affinities. The value for $Cu(O_2)$ is from ref 11.

all the CuO_x species observed in the current work as well as their EAs. Essentially, three types of structures are formed: (1) oxides, CuO, OCuO, $OCuO_2$; (2) Cu/O_2 complexes, $Cu(O_2)$, $Cu(O_2)_2$, $Cu(O_2)_3$; and (3) O_2-solvated oxides, $(OCuO)(O_2)$, $(OCuO)(O_2)_2$, $(OCuO_2)(O_2)$. The $Cu(O_3)$ may be considered as a fourth structure. Many of these structures are not known except CuO and $Cu(O_2)$, and those shown in Figure 12 are only proposals. However, the agreement between our PES spectrum shown in Figure 3 and the MO scheme of a linear OCuO gives strong support for the linear structure.[11] The $Cu(O_2)$ complex has been studied extensively previously.[3-7,10] The most recent calculation predicted that it has a C_{2v} ground state (side-on structure) as shown in Figure 12.[10] On the basis of this, we draw all the Cu/O_2 complexes as side-on bonding, including $OCuO_2$. $Cu(O_2)_2$ has been observed previously in low-temperature matrix experiments, and end-on types of structures have been proposed.[6] This same study also observed the $Cu(O_3)$ complex.

Copper plays an important role in biological dioxygen metabolism.[2] The $Cu(O_2)$ complex was viewed as the simplest model to study the $Cu-O_2$ interactions. However, in biological systems, the Cu atom is always complexed with other ligands, and the O_2 molecule is only one of them. Therefore, the new Cu/O_2 complexes observed currently may serve as more realistic models to study the $Cu-O_2$ interactions relevant to biological O_2 transport or activation of O_2 by Cu.

The oxidation states of the Cu atom in the CuO_x series are also interesting. Although in bulk CuO oxide the Cu and O atoms both have oxidation states of two,[1] we see in the isolated CuO diatomic molecule each is of oxidation state one,[8] while the molecule with oxidation state two ($Cu^{2+}O^{2-}$) is significantly higher in energy (Figure 11). The high oxidation states are stabilized in the bulk because of the Madelung energies or the multiple coordination in the crystal. Interestingly, this effect may already manifest itself in the rhombus CuO dimer (Cu_2O_2), in which the Cu and O atoms can be regarded as in oxidation states of two.[24] As x increases from 1 to 2 in CuO_x, the Cu atom can be considered to be in +2 oxidation state in the OCuO molecule although the O atoms are still in the −1 oxidation state. Oxidation state of +3 is rare for Cu although it is known to exist in ternary oxide such as $KCuO_2$ or high-temperature superconductors.[1,25] Therefore, the oxidation state of Cu in CuO_3 is not expected to be higher than +2. The molecule adapts to this by forming an O−O bond, as shown in Figure 12. Effectively, the Cu atom should still be viewed as +2 in CuO_3, in which the O_2 resembles a superoxide group.

As x further increases in CuO_x, we see either O_2 complexes or O_2-solvated oxide clusters. The latter are probably formed during the supersonic expansion where the O_2 molecules in the carrier gas condense onto the smaller CuO_x^- species. This seems to be particularly efficient for the copper oxide systems, since we have not observed such O_2-solvated oxide clusters among the other transition metal cluster systems under similar experimental conditions.[26]

V. Summary

We report an extensive anion photoelectron spectroscopic study of novel CuO_x ($x = 0-6$) species. PES spectra of all the species are obtained at various detachment photon energies ranging from 2.33 to 6.42 eV. It is shown that the various photon energy PES spectra provide several advantages, including (1) low photon energies give better spectral resolution, (2) high photon energies allow species with high EAs to be studied and reveal more excited states of the neutrals, (3) photon energy-dependent detachment cross sections help spectral assignments, and (4) observations of photon energy-dependent anion dissociation.

For the Cu^- atomic anion, we observe an intense two-electron detachment transition to the ^2P excited state of the Cu atom at 6.42 eV. For CuO^-, excited states of the anion are observed. We also observe transitions to the $Cu^{2+}O^{2-}$ excited states of CuO that show significant geometry changes from the anion ground state. A new CuO_2^- spectrum at 6.42 eV is presented that reveals all the six valence molecular orbitals of the linear OCuO molecule arising from the Cu 3d and O 2p orbitals. CuO_3^- is shown to have an $OCuO_2$ structure that dissociates at 355 nm to form an internally hot CuO^- plus O_2. We show that the electronic structure of the CuO_3 molecule can be considered to be due to that of CuO perturbed by an O_2. The CuO_5^- spectra are similar to that of CuO_3^-, and it is suggested to be a CuO_3 solvated by an O_2. For both CuO_4^- and CuO_6^- two isomers are observed. One of these dissociates at 355 nm to form Cu^- plus O_2. This isomer is a Cu/O_2 complex, $Cu(O_2)_{2,3}$. The other isomer gives spectra that are similar to that of the linear $OCuO^-$ molecule and is shown to be O_2-solvated $OCuO^-$, $(OCuO^-)(O_2)_{1,2}$. Theoretical works on these novel $Cu/O/O_2$ species observed in the current work would be extremely interesting in order to completely understand the copper−oxygen chemical bonding which is important in several areas of chemistry.

Acknowledgment. Support for this research from the National Science Foundation under Grant CHE-9404428 is

gratefully acknowledged. Development of the cluster apparatus was funded by Pacific Northwest National Laboratory and the U.S. Department of Energy, Office of Basic Energy Sciences, Chemical Science Division. The work is performed at Pacific Northwest National Laboratory, operated for the U.S. Department of Energy by Battelle under Contract DE-AC06-76RLO 1830.

References and Notes

(1) Cox, P. A. *Transition Metal Oxides*; Oxford: New York, 1995.

(2) Tyeklar, Z.; Karlin, K. D. *Acc. Chem. Res*. **1989**, *22*, 241. Halfen, J. A.; *et al*. *Science* **1996**, *271*, 1397.

(3) Brown, C. E.; Mitchell, S. A.; Hackett, P. A. *J. Phys. Chem*. **1991**, *95*, 1062.

(4) Vinckier, C.; Corthouts, J.; De Jaegere, S. *J. Chem. Soc*., *Faraday Trans. 2* **1988**, *84*, 1951.

(5) Sulzle, D.; Schwarz, H.; Moock, K. H.; Terlouw, J. K. *Int. J. Mass Spectrom. Ion Processes* **1991**, *108*, 269.

(6) Ozin, G. A.; Mitchell, S. A.; Garcia-Prieto, J. *J. Am. Chem. Soc*. **1983**, *105*, 6399.

(7) Tevault, D. E. *J. Chem. Phys*. **1982**, *76*, 2859. Bondybey, V. E.; English, J. H. *J. Phys. Chem*. **1984**, *88*, 2247. Howard, J. A.; Sutcliffe, R.; Mile, B. *J. Phys. Chem*. **1984**, *88*, 4351. Kasai, P. H.; Jones, P. M. *J. Phys. Chem*. **1986**, *90*, 4239. Mattar, S. M.; Ozin, G. A. *J. Phys. Chem*. **1988**, *92*, 3511.

(8) Langhoff, S. R.; Bauschlicher, C. W. *Chem. Phys. Lett*. **1986**, *124*, 241. Madhaven; P. V.; Newton, M. D. *J. Chem. Phys*. **1985**, *83*, 2337. Igel, G.; *et al*. *J. Chem. Phys*. **1984**, *81*, 2737. Bagus, P. S.; Nelin, C. J.; Bauschlicher, C. W. *J. Chem. Phys*. **1983**, *79*, 2975.

(9) Merer, A. J. *Annu. Rev. Phys. Chem*. **1989**, *40*, 407. Huber, K. P.; Herzberg, G. *Molecular Spectra and Molecular Structure. IV. Constants of Diatomic Molecules*; Van Nostrand Reinhold: New York, 1979.

(10) Hrusak, J.; Koch, W.; Schwarz, H. *J. Chem. Phys*. **1994**, *101*, 3898. Bauschlicher, C. W.; Langhoff, S. R.; Partridge, H.; Sodupe, M. *J. Phys. Chem*. **1993**, *97*, 856. Mochizuki, Y.; Nagashima, U.; Yamamoto, S.; Kashiwagi, H. *Chem. Phys. Lett*. **1989**, *164*, 225.

(11) Wu, H.; Desai, S. R.; Wang, L. S. *J. Chem. Phys*. **1995**, *103*, 4363.

(12) Ha, T. K.; Nguyen, M. T. *J. Phys. Chem*. **1985**, *89*, 5569.

(13) Polak, M. L.; Gilles, M. K.; Ho, J.; Lineberger, W. C. *J. Phys. Chem*. **1991**, *95*, 3460.

(14) Wang, L. S.; Cheng, H. S.; Fan, J. *J. Chem. Phys*. **1995**, *102*, 9480.

(15) Kruit, P.; Read, F. H. *J. Phys. E: Sci. Instrum*. **1983**, *16*, 313. Cheshnovsky, O.; Yang, S. H.; Pettiette, C. L.; Craycraft, M. J.; Smalley, R. E. *Rev. Sci. Instrum*. **1987**, *58*, 2131.

(16) Hufner, S. *Photoelectron Spectroscopy*; Springer-Verlag: New York, 1995; p 15.

(17) Moore, C. E. *Atomic Energy Levels*, Natl. Bur. Stand. Circ.; U.S. GPO: Washington DC, 1971; Vol. II.

(18) Suzer, S.; Lee, S. T.; Shirley, D. A. *Phys. Rev. A* **1976**, *13*, 1842.

(19) Fan, J.; Wang, L. S. *J. Phys. Chem*. **1994**, *98*, 11814. Fan, J.; Lou, L.; Wang, L. S. *J. Chem. Phys*. **1995**, *102*, 2701.

(20) Wu, H.; Wang, L. S. Unpublished results.

(21) Markovich, G.; Pollack, S.; Giniger, R.; Cheshnovsky, O. *J. Chem. Phys*. **1994**, *101*, 9344.

(22) Andersen, T.; Lykke, K. R.; Neumark, D. M.; Lineberger, W. C. *J. Chem. Phys*. **1987**, *86*, 1858.

(23) Gutowski, M.; Simons, J. *J. Chem. Phys*. **1994**, *101*, 4867; **1994**, *100*, 1308; *J. Phys. Chem*. **1994**, *98*, 8326.

(24) Wang, L. S.; Wu, H.; Desai, S. R.; Lou, L. *Phys. Rev. B* **1996**, *53*, 8028.

(25) Burdett, J. K.; Sevov, S. *J. Am. Chem. Soc*. **1995**, *117*, 12788.

(26) Wu, H.; Desai, S. R.; Wang, L. S. *J. Am. Chem. Soc*. **1996**, *118*, 5296.